

# Application of Ion Trap-MS with H/D Exchange and QqTOF-MS in the Identification of Microbial Degradates of Trimethoprim in Nitrifying Activated Sludge

Peter Eichhorn,<sup>\*,†</sup> P. Lee Ferguson,<sup>‡</sup> Sandra Pérez,<sup>†</sup> and Diana S. Aga<sup>†</sup>

Chemistry Department, The State University of New York at Buffalo, 611 Natural Sciences Complex, Buffalo, New York 14260, and Department of Chemistry and Biochemistry, University of South Carolina, 631 Sumter Street, Columbia, South Carolina 29208

In this work, the identification of two microbial degradation products of the antimicrobial trimethoprim (290 Da) is described. The structural elucidation of the metabolites, which were produced by nitrifying activated sludge bacteria in a small-scale laboratory batch reactor, was accomplished by electrospray ionization–ion trap mass spectrometry conducting consecutive fragmentation steps (MS<sup>n</sup>) combined with H/D-exchange experiments. Although one metabolite corresponded to  $\alpha$ -hydroxytrimethoprim (306 Da), oxidation of the aromatic ring within the diaminopyrimidine substructure was determined for the second degradate (324 Da). Accurate mass measurements of the two metabolites were provided by a hybrid quadrupole time-of-flight-mass spectrometer operated in MS/MS mode. With absolute mass errors of <5 mDa, it allowed us to confirm the proposed elemental composition for the protonated precursor ions as well as for a series of fragment ions that were previously identified by ion trap mass spectrometry. The study emphasized the potential of nitrifying activated sludge bacteria for breaking down an environmentally relevant pharmaceutical that is otherwise poorly degradable by a bacterial community encountered in conventional activated sludge.

The widespread occurrence of persistent residues of pharmacologically active compounds in natural aquatic environments has received considerable attention in the past few years.<sup>1–3</sup> Since most pharmaceuticals used in human medicine are eventually disposed of with the sewage, wastewater treatment facilities play a key role in removing drugs from the water stream, thus preventing them from reaching the receiving water bodies. Those compounds that have a low tendency to partition onto biosolids and are not amenable to microbial degradation during biological treatment using activated sludge possess the greatest potential of surviving

the treatment plant. Among the frequently detected drugs in surface waters is trimethoprim,<sup>4–6</sup> an antimicrobial compound of high water solubility that is commonly prescribed in combination with the sulfonamide sulfamethoxazole for the treatment of infectious diseases in humans. Regarding the fate of trimethoprim during sewage treatment, analytical measurements on composite samples of primary and secondary effluents from two sewage treatment plants in Switzerland showed that the antimicrobial was eliminated only to a small extent during the conventional activated sludge process. While in one plant the trimethoprim concentration dropped by 24%, no measurable removal was reported for a second facility studied.<sup>7</sup> The lacking capability of the bacterial consortium in activated sludge to metabolize trimethoprim was corroborated in laboratory settings. In experimental setups designed to simulate the biological wastewater treatment, trimethoprim exhibited a strong resistance to microbial breakdown by activated sludge bacteria, even after a prolonged adaptation phase of several weeks.<sup>8,9</sup>

In contrast to this recalcitrance in typical wastewater treatment plants, a rapid primary degradation of trimethoprim was achieved in nitrifying activated sludge collected from a municipal sewage treatment plant employing a two-stage process composed of an activated sludge coupled to a nitrification process.<sup>8</sup> Such distinct capability of nitrifying bacteria to degrade recalcitrant compounds has been reported in several studies for a wide array of aromatic xenobiotics, for example, anisol,<sup>10</sup> aniline,<sup>11</sup> and naphthalene,<sup>12</sup> in which ammonia-oxidizing bacteria (AOB), producing an ammonia

\* Corresponding author. Phone: 1-716-645-6800, x2206. Fax: 1-716-645-6963. E-mail: Peter.Eichhorn@HispaVista.com.

<sup>†</sup> The State University of New York at Buffalo.

<sup>‡</sup> University of South Carolina.

(1) Heberer, T. *Toxicol. Lett.* **2002**, *131*, 5–17.

(2) Ternes, T. A.; Joss, A.; Siegrist, H. *Environ. Sci. Technol.* **2004**, *38*, 392A–399A.

(3) Ternes, T. A. *TrAC, Trends Anal. Chem.* **2001**, *20*, 419–434.

(4) Hilton, M. J.; Thomas, K. V. *J. Chromatogr., A* **2003**, *1015*, 129–141.

(5) Stackelberg, P. E.; Furlong, E. T.; Meyer, M. T.; Zaugg, S. D.; Henderson, A. K.; Reissman, D. B. *Sci. Total Environ.* **2004**, *329*, 99–113.

(6) Vanderford, B. J.; Pearson, R. A.; Rexing, D. J.; Snyder, S. A. *Anal. Chem.* **2003**, *75*, 6265–6274.

(7) Goebel, A.; McArdell, C. S.; Suter, M. J. F.; Giger, W. *Anal. Chem.* **2004**, *76*, 4756–4764.

(8) Pérez, S.; Eichhorn, P.; Aga, D. S. *Environ. Toxicol. Chem.* **2005**, *24*, in press.

(9) Junker, T.; Knacker, T.; Römbke, J.; Alexy, R.; Kümmerer, K. Proceedings of the 24th Annual Meeting SETAC in North America, Austin TX, November 8–13, 2003.

(10) Chang, S. W.; Hyman, M. R.; Williamson, K. J. Proceedings of the 5th International In Situ and On-Site Bioremediation Symposium, San Diego CA, Apr. 19–22, 1999; pp 131–135.

(11) Keener, W. K.; Arp, D. J. *Appl. Environ. Microbiol.* **1994**, *60*, 1914–1920.

(12) Chang, S. W.; Hyman, M. R.; Williamson, K. J. *Biodegradation* **2003**, *13*, 373–381.

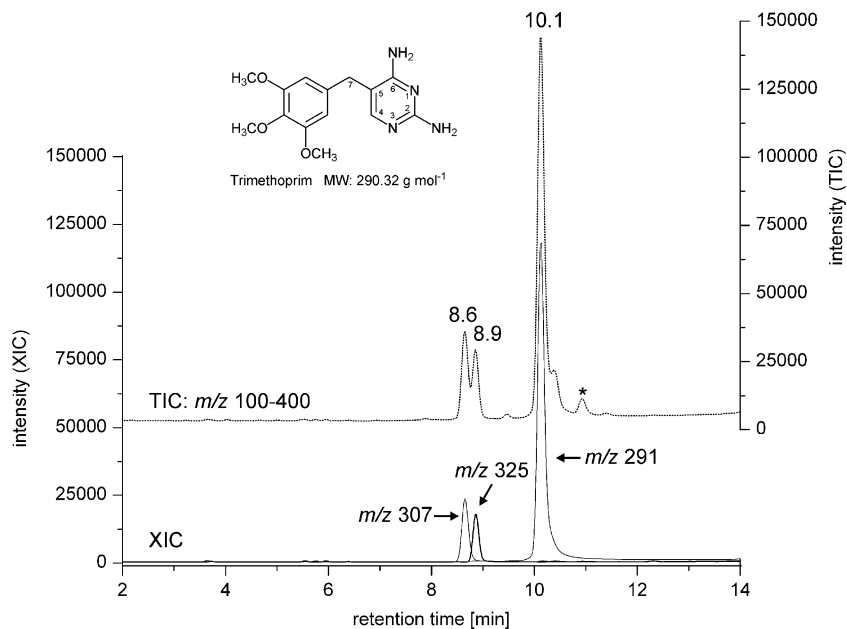


**Figure 1.** LC/ESI-MS chromatogram corresponding to sample from batch reactor spiked with trimethoprim at 20 mg/L. Upper mass trace shows total ion chromatogram (TIC) acquired over mass range of  $m/z$  100–400 in positive ion mode. Extracted ion chromatograms (XIC) are shown in the lower part of the graph. The peak in the TIC marked with an asterisk was identified as an impurity in the trimethoprim used (carrying an ethoxy group instead of a methoxy group;  $m/z$  305).

monooxygenase enzyme of broad specificity, were suggested to co-metabolize the organic substrates. The assumption of AOB being involved in the biotransformation process of the pollutants was supported by findings that the degradation was inhibited in the presence of specific AOB inhibitors and that the observed metabolites were compatible with reactions catalyzed by ammonia monooxygenase.

To gain insight into the degradation processes of the antimicrobial trimethoprim that are brought about by bacteria specific to nitrifying activated sludge, this study aimed at the identification and characterization of major metabolites of the target compound. To this end, the structures of biodegradation products, previously generated in a small-scale laboratory batch reactor, were elucidated by applying multiple-stage fragmentation studies in combination with H/D-exchange experiments using an electrospray ionization–ion trap mass spectrometer (ESI-IT-MS). In addition, a quadrupole time-of-flight-mass spectrometer (ESI-QqTOF-MS) was used to provide accurate mass measurements, allowing verification of the assigned chemical structures of the metabolites.

## EXPERIMENTAL SECTION

**Chemical Standards.** Trimethoprim (CAS no. 738-70-5) was purchased from Riedel de Haën (Seelze, Germany). The organic solvents acetonitrile and methanol were ACS grade (Burdick & Jackson, Muskegon, MI). Water was prepared with a Nanopure Diamond water purifier (Barnstead, Dubuque, IA). Deuterium oxide was obtained from Cambridge Isotopes Laboratories Inc. (Andover, MA). Acetic acid- $d_4$  was purchased from Aldrich (St. Louis, MO).

**Biodegradation Experiments.** An amber 4-L glass bottle was loaded with 4 L of nitrifying activated sludge, freshly collected from the nitrification tank of a municipal sewage treatment plant (Amherst, NY). Bubbling of air through Teflon tubing into the test medium provided aeration of the system and suspension of

the sludge particulate matter. The biodegradation of trimethoprim was studied at two test concentrations: (a) at 20 mg/L for the preparation of sufficient material required for the mass spectrometric characterization of the metabolites and (b) at 20  $\mu$ g/L for obtaining a degradation profile at an environmentally relevant concentration of trimethoprim.

**LC/ESI-MS Analysis.** The liquid chromatograph used in this study was an Agilent Series 1100 comprising the modular components: quaternary pump, a micro vacuum solvent degasser, and an autosampler with a 100-well tray. Separations were achieved on a Thermo Hypersil-Keystone BetaBasic-18 100  $\times$  2.1 mm (3  $\mu$ m) column equipped with a 10  $\times$  2.1 mm guard column of the same packing material. The mobile phases were (A) water acidified with 0.3% formic acid and (B) acetonitrile. The gradient program started from 95 A/5% B. After 1 min, the portion of A was linearly decreased to 57% within 10.0 min and further to 5% within 0.1 min. The latter condition was held for 3.9 min. The initial mobile phase composition was restored within 0.1 min and maintained for column regeneration for another 5.9 min, resulting in a total run time of 20 min. The flow rate was 250  $\mu$ L/min, and the injection volume was 20  $\mu$ L. During the first 1.8 min and the last 5.9 min of each chromatographic run, the LC stream exiting the analytical column was directed to the waste via a programmable switching valve integrated in the mass spectrometer. The mass spectrometric analysis was performed on an Agilent Series 1100 SL single-quadrupole instrument equipped with an ESI source. All acquisitions were performed under positive ionization mode with a capillary voltage of +4000 V. Nitrogen was used as nebulizer gas (35 psi) as well as drying gas at a temperature of 350  $^{\circ}$ C (10 L/min). For quantitative analysis of trimethoprim and its metabolites, data were acquired in selected ion monitoring (SIM) mode recording the protonated molecules,  $[M + H]^+$ , of trimethoprim ( $m/z$  291), the metabolite M306 ( $m/z$  307), and the

metabolite M324 ( $m/z$  325) using fragmentor values of 140. The ions  $m/z$  261, 289, and 181, which represented the most intense fragment ions detected at a fragmentor value of 230, were used as qualifier ions for trimethoprim, M306 and M324, respectively. Data acquisition and processing was done with the software Chemstation Rev. A.09.03.

**LC/ESI-IT-MS Analysis.** The ThermoFinnigan system used for multiple-stage MS experiments consisted of the following components: Surveyor pump, Surveyor autosampler, and LCQ Advantage ion trap mass spectrometer, equipped with an ESI interface. The analytical column, mobile phase composition, and gradient elution were the same as described above for the single-quad MS except for the H/D-exchange experiments, for which mobile phase A was  $D_2O$  containing 0.3%  $CD_3COOD$ . The flow rate was 200  $\mu L/min$ ; the injection volume was 10  $\mu L$ . The needle voltage of the ESI interface was set to +5000 V, the sheath gas flow was 30, the temperature of the ion transfer tube was 300  $^{\circ}C$ , and the capillary voltage was 10 V. For MS<sup>n</sup> experiments, precursor ions were selected with an isolation width of 1.5 Da, except for the analysis of H/D-exchanged analytes, for which the isolation width was set to 1.0 Da. Relative collision energies were between 25 and 40%. Helium was used as both damping gas and collision gas at a pressure of  $\sim 1$  mTorr.

**LC/ESI-QqTOF-MS Analysis.** Accurate mass MS and MS/MS analysis of trimethoprim metabolites was performed using a Waters/Micromass Q-TOF API-US system coupled to an Agilent 1100 Nanobore HPLC system. Diluted batch reactor samples were separated on an Agilent Zorbax 300SB-C18 nanobore column (150  $\times$  0.1 mm, 3.5- $\mu m$  particles) prior to MS analysis. The mobile phases were (A) water acidified with 0.1% formic acid and (B) acetonitrile with 0.1% formic acid. The flow rate was 500 nL/min, with a gradient beginning at 95% A/5% B for 2 min and increasing linearly to 5% A/95% B over 10 min. The injection volume was 0.5  $\mu L$ . The column was directly interfaced to the nanoelectrospray ion source using a tapered fused-silica electrospray emitter (New Objective), and the required electrospray voltage (+2800 V) was applied through the stainless steel column endfitting. External mass calibration was performed just prior to analysis using  $Na-(NaTFA)_n^+$  clusters from 50  $\mu M$  sodium trifluoroacetate in 50:50 acetonitrile/water. This calibrant was also used as a source of reference internal lock mass ( $m/z$  = 430.9142) for accurate mass measurement of precursor and product ions from the trimethoprim metabolites. The instrument was operated at a resolution of 10 000 (fwhm), and (+)ESI mass spectra were acquired at 1-s intervals. High-resolution product ion spectra of M306 and M324 metabolites were acquired using argon as a CID gas with collision energies of 25 eV.

**Sample Preparation.** Samples collected from the batch reactor amended with trimethoprim at a concentration of 20  $\mu g/L$  were centrifuged for 4 min at 12000g. An aliquot of the supernatant was injected into the LC/ESI-MS without further treatment. For structural elucidation of the degradation products employing LC/ESI-IT-MS and LC/ESI-QqTOF-MS, a 100-mL sample from the batch reactor spiked at 20 mg/L was preconcentrated by solid-phase extraction (SPE). The sample was first filtered (1.2- $\mu m$  glass fiber) and then loaded onto a 6-mL/500-mg OASIS hydrophilic-lipophilic (HLB) SPE cartridge (Waters, Milford, MA) coupled in tandem to a 6-mL/500-mg Sep-Pak tC18 SPE cartridge (Waters).

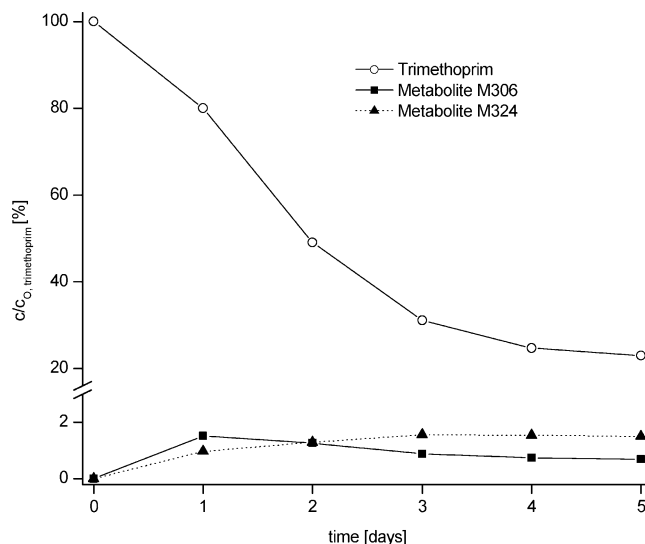


**Figure 2.** Degradation profile of trimethoprim in batch reactor. Nitrifying activated sludge was amended with 20  $\mu g/L$  of the test compound.

This combination of two different sorbent materials was used to ensure high recoveries of the metabolites. The dried cartridges were eluted separately with 3  $\times$  2 mL of methanol, and the combined eluates were evaporated to dryness under a gentle stream of nitrogen. The residue was reconstituted in 1 mL of 10% acetonitrile/90% water. For the H/D-exchange study, a second batch-reactor sample was processed in the same way as described above using SPE. The dried residue, however, was taken up in 1 mL of 10% acetonitrile/90%  $D_2O$  which contained 0.3%  $CD_3COOD$  as catalyst for the H/D exchange.

**Quantification.** To determine the concentration of trimethoprim and to estimate those of its two metabolites in the samples from the batch reactor spiked at 20  $\mu g/L$ , external calibration with trimethoprim as reference substance was performed for all three compounds over a linear range from 0.02 to 25  $\mu g L^{-1}$ , with the assumption that they have identical ionization efficiencies and response factors. In view of the relatively narrow retention time range and the structural similarities enabling protonation at the amino group, this approach provided a reasonable estimate for the metabolite levels. As far as matrix ionization suppression or enhancement effects were concerned, this issue had been addressed in a previous work of our group comparing possible matrix effects in different types of waters analyzed on the Agilent LC/ESI-MS.<sup>8</sup> Preparation of the calibration series in distilled water versus not-concentrated sewage had shown no significant impact on the relative signal intensity for trimethoprim and a series of sulfonamide antibiotics.

## RESULTS AND DISCUSSION

**Degradation of Trimethoprim.** To investigate the microbial degradation of trimethoprim in a nitrification tank, a batch reactor loaded with freshly collected nitrifying activated sludge was spiked with the parent compound at a concentration of 20 mg/L. Such high a concentration was chosen to allow the detection of novel metabolites in solution. Screening of the reactor samples by LC/ESI-MS over a scan range from  $m/z$  100 to 400 showed the emergence of two peaks at 8.6 and 8.9 min as the signal of

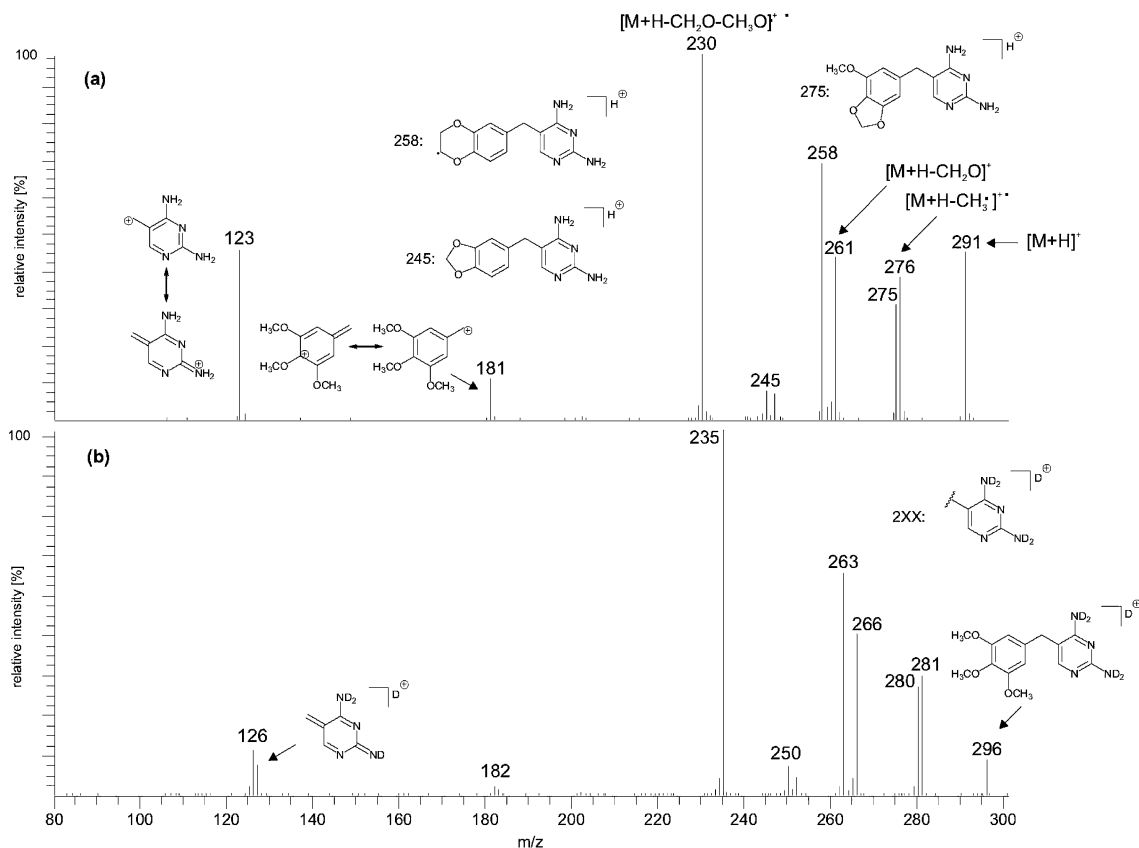


**Figure 3.** (a) (+)-ESI-MS<sup>2</sup> spectrum of protonated trimethoprim,  $[M + H]^+ = m/z 291$ ; and (b) (+)-ESI-MS<sup>2</sup> spectrum of trimethoprim after H/D exchange,  $[M(D_4) + D]^+ = m/z 296$ .

trimethoprim (10.0 min) disappeared (Figure 1). These two peaks, which were not observed in the control batch reactor loaded with sterilized sewage, had molecular ions,  $[M + H]^+$ , of  $m/z$  307 and 325 (metabolites termed as M306 and M324). On the basis of the order of elution in the reversed-phase column (Figure 1), it was deduced that the microbial transformation of trimethoprim resulted in more polar products, suggesting an oxidative breakdown of the antibiotic. A second experiment with a test concentration of 20  $\mu\text{g/L}$  was carried out to illustrate that the degradation route was independent of the initial concentration of trimethoprim. Compound-specific analysis by LC/ESI-MS operated in SIM mode provided the degradation profile depicted in Figure 2. The instant decline of the trimethoprim concentration without lag phase was paralleled by the concurrent formation of the metabolites M306 and M324, suggesting that both compounds were primary degradation products from the direct transformation of the parent drug. As can be seen in Figure 2, the transformation rate of trimethoprim decreased considerably after 2 days, and by day 5, a steady level was attained with  $\sim 25\%$  of the starting material remaining undegraded. As to possible elimination of trimethoprim from the liquid phase through adsorption onto the sludge, previous studies conducted in identical reactor settings proved this removal pathway to be insignificant.<sup>8</sup> Regarding the two transient metabolites, they built up to a relatively constant concentration of  $\sim 2\%$  of the initial trimethoprim, indicating that they were subject to further degradation. Adsorption of the intermediates onto the biomass was unlikely in view of the increase in polarity relative to the parent compound. The incomplete primary degradation of trimethoprim—also observed in the 20 mg/L experiment—was

attributed to the gradual acidification of the test medium from the initial of pH 7.2 down to 4.8 by day 5. This was due to the acid-producing nitrification process, that is, the oxidation of ammonium to nitrate. Because the optimal pH range for nitrifying bacteria is between 7.5 and 8.6,<sup>13</sup> the considerable decrease of the pH resulted in a strong reduction of the metabolic activity of those microorganisms involved in the degradation of trimethoprim. A complete degradation of trimethoprim, however, was achieved when the pH of the test liquor was maintained in the slightly alkaline range using ammonium hydroxide for adjusting the pH (data not shown).

**Structure Elucidation.** As far as the fragmentation pattern of the parent drug trimethoprim is concerned, selection of the protonated precursor ion ( $m/z$  291) in the ion trap and subsequent activation resulted in the (+)-ESI-MS<sup>2</sup> spectrum shown in Figure 3a. All of the fragment ions with  $m/z$  values between 230 and 276 were based on a structure comprising the benzene ring, the bridging methylene group, and the intact diaminopyrimidine. That the latter moiety did not undergo any fragmentation under the conditions applied was corroborated by the MS<sup>2</sup> spectrum of the H/D-exchanged trimethoprim ( $[M(D_4) + D]^+$  at  $m/z$  296), which contained a total of four exchangeable hydrogen atoms in the amino groups (Figure 3b). The increment of the ion masses by five units ( $m/z$ 's 230  $\rightarrow$  235, 245  $\rightarrow$  250, 258  $\rightarrow$  263, 261  $\rightarrow$  266, 275  $\rightarrow$  280, and 276  $\rightarrow$  281) indicated that the two deuterated amino groups ( $-\text{ND}_2$ ) were present in all of these fragment ions. The structures of the ions  $m/z$  230, 261, and 275, as depicted in

(13) Albertson, O. E. *Nutrient Control – Manual of Practice FD-7 Facilities Design*; Water Pollution Control Federation: Alexandria, VA, 1983.



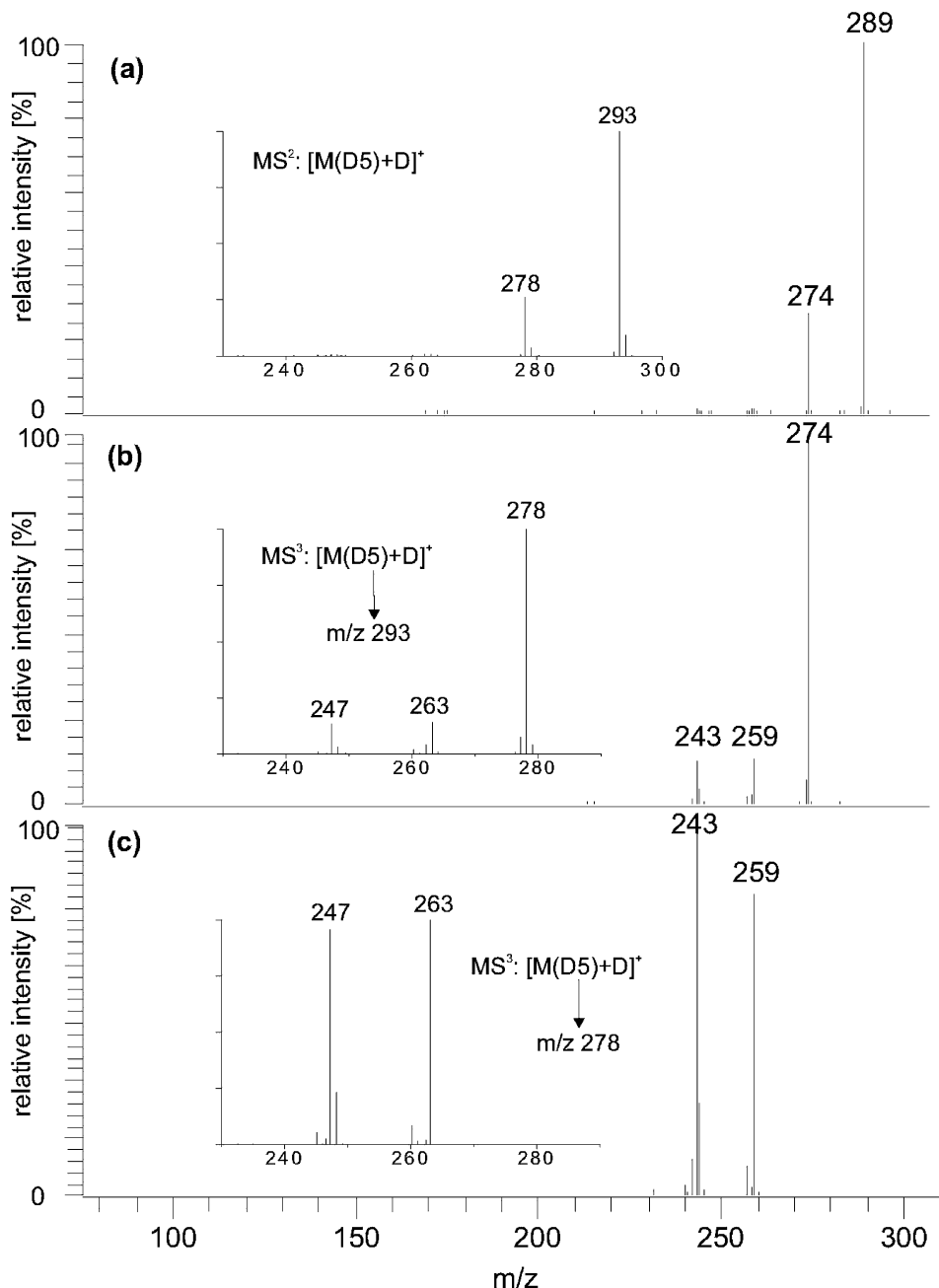


**Figure 4.** (a) (+)-ESI-MS<sup>2</sup> spectrum of metabolite M306 ( $m/z$  307); (b) (+)-ESI-MS<sup>3</sup> spectrum of metabolite M306 ( $m/z$  307  $\rightarrow$  289); and (c) (+)-ESI-MS<sup>3</sup> spectrum of metabolite M306 ( $m/z$  307  $\rightarrow$  274). Insets show analogous spectra of M306 after H/D exchange ( $[M(D5) + D]^+ = m/z$  313).

Figure 3a, were consistent with those proposed by Barbarin et al.<sup>14</sup> for the fragmentation pathway of trimethoprim in a triple-quadrupole mass spectrometer. The structures suggested for the three ions with  $m/z$  245, 258, and 276 (Figure 3a) derived from losses and rearrangements within the trimethoxybenzene portion. In addition to the assigned product ions encompassing both aromatic rings, two further fragment ions,  $m/z$  181 and 123, were observed arising from the cleavage of the protonated molecule at either side of the central methylene group (C7 atom; see Figure 1 for atom numbering).<sup>14</sup> Stabilization of the positive charge could be readily achieved through mesomeric resonance across the trimethoxybenzene and diaminopyrimidine rings, respectively (possible structures shown in Figure 3a).

(14) Barbarin, N.; Henion, J. D.; Wu, Y. J. *Chromatogr., A* **2002**, *970*, 141–154.

Of the two metabolites produced in the nitrifying activated sludge, M306, eluting in the LC chromatogram 1.5 min prior to trimethoprim (see Figure 1), had a molecular weight of 16 Da ( $[M + H]^+$ ,  $m/z$  307) higher than trimethoprim, suggesting that the antibiotic had undergone an oxidative transformation; i.e., the degradate formed was bearing an additional oxygen atom. In contrast to the signal-rich mass spectrum of the parent compound, the product ion profile of  $m/z$  307 generated in the IT-MS merely displayed two fragment ions: a base peak at  $m/z$  289 and a less intense ion at  $m/z$  274 (Figure 4a). The neutral loss of 18 Da, presumably the expulsion of water, appeared to be strongly favored over other fragmentation processes involving cleavages from the methoxy moieties, as observed for trimethoprim (see Figure 3a). Confirming evidence that the loss of 18 Da was due

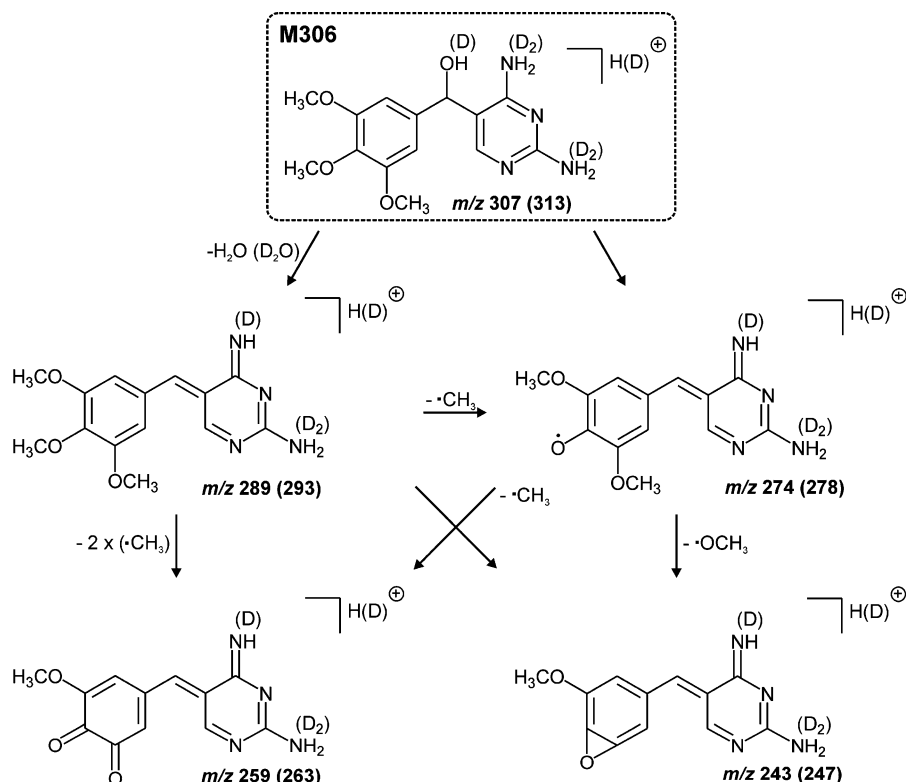


**Figure 5.** Proposed fragmentation pathway of the protonated M306 under (+)-ESI conditions (ion masses obtained for H/D-exchanged molecule in parentheses).

to water was provided by the (+)-ESI-MS<sup>2</sup> spectrum of M306 after H/D exchange. First, the deuterium adduct,  $[M + D]^+$ , was detected at  $m/z$  313; i.e., the microbial conversion of trimethoprim had increased the number of exchangeable protons in the molecule by one, for which a hydroxy group could account. Second, the MS<sup>2</sup> spectrum of  $m/z$  313 (inset in Figure 4a) showed a fragment ion at  $m/z$  293, which was consistent with the elimination of D<sub>2</sub>O (20 Da). To eliminate water from the protonated molecule of the metabolite M306, the C–H bond subject to oxidation had to be located such that formation of a double bond was feasible upon expulsion of water. Thus, transformation of an N–H bond to N–OH could be ruled out, since it would not alter the number of exchangeable protons. Only the C–H bond of the methylene group (C7 atom) linking the trimethoxybenzene to the diaminopyrimidine met this requirement, whereas oxidation of one of the methoxy groups or of an aromatic C–H bond could be excluded, since the resulting hydroxy group would lack a hydrogen on the  $\beta$ -atom essential for formation of a double bond. The driving force behind the elimination of water during resonance excitation in the ion trap was hypothesized to be formation of a conjugated system ( $m/z$  289) extending over both rings, as depicted in Figure 5. As for the fragment ion  $m/z$  274 (Figure 4a) differing from  $m/z$  289 by 15 Da, it was assigned to the loss of a methyl radical in analogy to the generation of  $m/z$  276 from the protonated trimethoprim (see MS<sup>2</sup> spectrum in Figure 3a). While the detection of the ion  $m/z$  278 in the spectrum of the H/D-exchanged M306 (inset in Figure 4a) confirmed that the neutral fragment expelled did not carry any exchangeable protons, the detection of  $m/z$  274 in the MS<sup>3</sup> spectrum of  $m/z$  307  $\rightarrow$  289 proved that this ion could be formed by  $m/z$  289, that is, by the precursor ion  $[M + H - H_2O]^+$  (Figure 4b). The product scan of

$m/z$  289 did not generate any fragment ions originating from a central cleavage of the molecule, emphasizing the particular stability of the aromatic structure of all fragment ions presented in Figure 5. The structural identification of the two ions with  $m/z$  259 and 243 that were detected in the product ion profile of  $m/z$  289 (Figure 4b) was accomplished by performing an MS<sup>3</sup> scan on the sequence  $m/z$  306  $\rightarrow$  274 (Figure 4c). Plausible structures of the ions  $m/z$  259 and 243 were traced back to the elimination of a methyl radical and a methoxy radical, respectively. This interpretation was in agreement with the  $m/z$  values of the fragment ions in the analogous MS<sup>3</sup> spectra acquired for the H/D-exchanged M306 ( $m/z$  313  $\rightarrow$  278, inset in Figure 4c). The structures proposed for the ions  $m/z$  259 and 243 in Figure 5 were also consistent with the ion profile of the MS<sup>4</sup> scan on  $m/z$  306  $\rightarrow$  289  $\rightarrow$  259 (spectrum not shown). The ion  $m/z$  243 was not detected in this spectrum, because the *o*-benzoquinone structure of  $m/z$  259 could not readily give rise to the benzooxirene structure in the ion  $m/z$  243.

As far as the metabolite M324 is concerned, its molecular weight was 34 Da higher relative to trimethoprim (molecular weight = 290 Da), indicating oxidation or addition of a functional group. Isolation and activation of the protonated molecule,  $m/z$  325, yielded the (+)-ESI-MS<sup>2</sup> spectrum shown in Figure 6a. Detection of the base peak ion at  $m/z$  181, likewise observed in the product ion profile of the protonated trimethoprim, indicated that the trimethoxybenzene portion of the molecule had not undergone any structural modifications. The strong abundance of  $m/z$  181, as compared to its intensity in the trimethoprim spectrum, suggested its formation is favored over other fragmentation processes. Upon cleavage of the C5–C7 bond, conservation of the positive charge in the other part of the molecule resulted

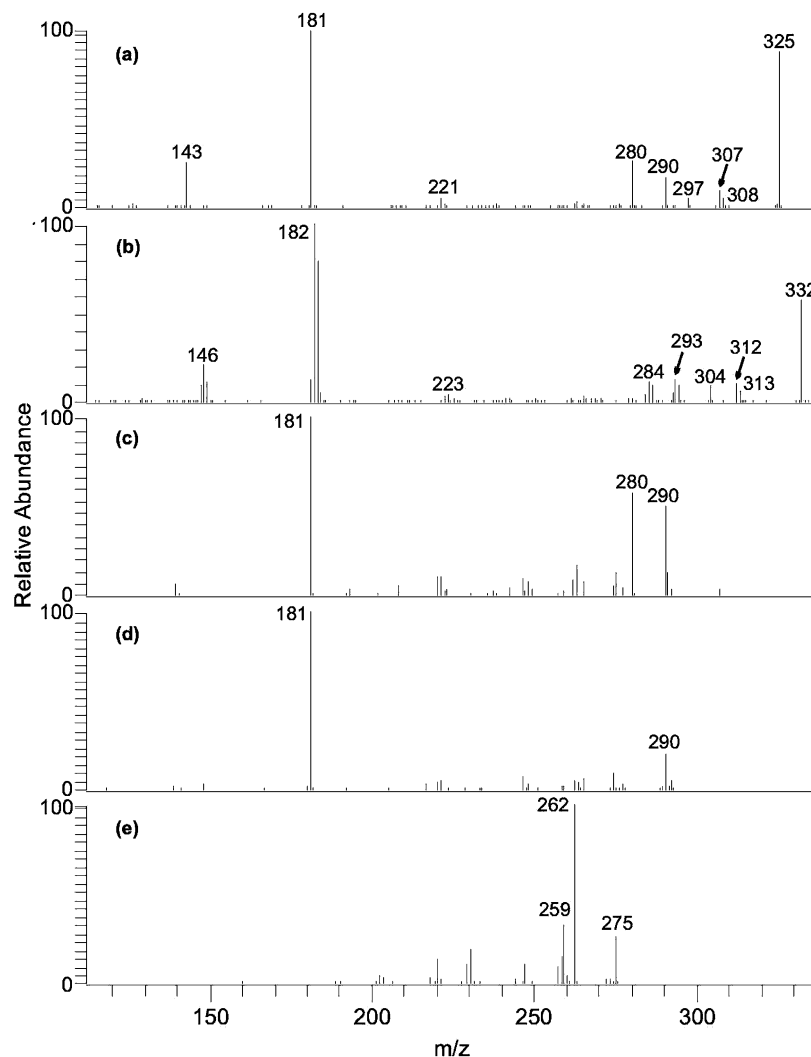


**Figure 6.** (a) (+)-ESI-MS<sup>2</sup> spectrum of protonated M324,  $[M + H]^+ = m/z$  325; (b) (+)-ESI-MS<sup>2</sup> spectrum of M324 after H/D exchange,  $[M(D_6) + D]^+ = m/z$  332; (c) M324, (+)-ESI-MS<sup>3</sup> of  $m/z$  325  $\rightarrow$  308; (d) M324, (+)-ESI-MS<sup>3</sup> of  $m/z$  325  $\rightarrow$  307; and (e) M324: (+)-ESI-MS<sup>3</sup> of  $m/z$  325  $\rightarrow$  290.

in the formation of the fragment ion  $m/z$  143. Unlike the ion  $m/z$  123 of trimethoprim including the heterocyclic ring, the ion  $m/z$  143 did not comprise the methylene group, suggesting that the C5-atom of the former diaminopyrimidine ring was a quaternary carbon atom, because in this instance, the loss of the aromatic structure of this ring would disable the stabilization of the positive charge, as postulated for  $m/z$  123 (for mesomeric structures see Figure 3a). The two fragment ions  $m/z$  308 and 307 were attributed to losses of ammonia and water, respectively, implying that the metabolite contained both an aliphatic hydroxy group (as in M306) and an aliphatic amino group (no loss of ammonia was observed for the aromatic amino groups in trimethoprim and M306). Unless an additional amino group had been introduced into the molecule by the action of nitrifying bacteria, the diaminopyrimidine ring lost its aromaticity as just put forward. Evidence for the presence of the aliphatic  $-OH$  and  $-NH_2$  groups was provided by the product ion scan of the H/D-exchanged M324. On one hand, the deuterated adduct ion,  $[M + D]^+$ , of this species was detected at  $m/z$  332 (Figure 6b); i.e., this molecule was bearing six exchangeable protons, as compared to four in trimethoprim; whereas one of the two exchangeable protons was

assigned to the hydroxy group, the second could be explained as a consequence of the loss of aromaticity converting the N1-atom or N3-atom into a secondary nitrogen atom. On the other hand, the fragment ion detected at  $m/z$  312 ( $\Delta m/z = 20$ ) was assigned as the elimination of  $D_2O$ ,  $ND_3$ , or both. The observation of  $m/z$  313, that is, the neutral loss of 19 Da, indicated that a non-acidic hydrogen could be abstracted during the fragmentation process, leading to the expulsion of  $HOD$ ,  $HND_2$ , or both. A probable position of the hydroxy group was at the C5-atom.

A further key fragment in the structural elucidation of M324 was the ion  $m/z$  297 (in the H/D-exchanged spectrum at  $m/z$  304). The mass difference between the precursor and the product ion of 28 Da in both spectra in Figure 6a and b proved that this fragment did not contain any exchangeable hydrogen atoms. Of the four possible elemental compositions,  $CH_2CH_2$ ,  $CH_2N$ ,  $N_2$ , and  $CO$ , the former three appeared to be rather unlikely to originate from M324. That  $CO$  in turn did not originate from a methoxy substituent in the benzene ring, but from a loss out of the structurally modified pyrimidine ring, was shown by generating the (+)-MS<sup>3</sup> spectrum of  $m/z$  325  $\rightarrow$  297, in which  $m/z$  181 represented a major fragment ion (spectrum not shown). A

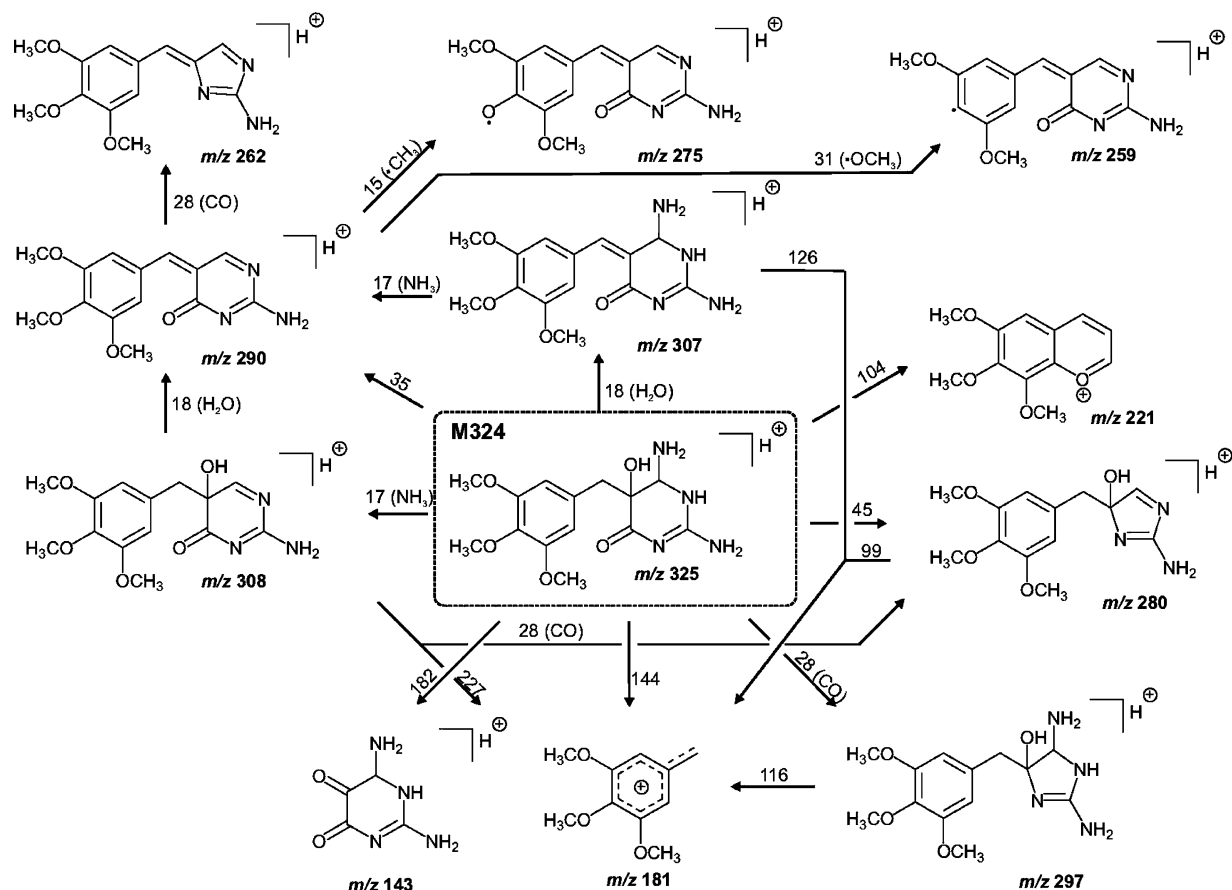


**Figure 7.** Major fragmentation routes of protonated M324 under (+)-ESI conditions as obtained by multiple-stage experiments.

plausible explanation for the expulsion of CO was derived from the oxidation of the C4-atom because this was the only secondary carbon atom in the ring. The loss of CO from a lactame ( $m/z$  290  $\rightarrow$  262, Figure 6e) was then feasible under ring contraction, yielding a five-membered ring (Figure 7). Regarding the fragment ion  $m/z$  290 observed in the MS<sup>2</sup> spectrum of  $[M + H]^+$  of M324 (Figure 6a), its identity could be determined by acquiring the (+)-ESI-MS<sup>3</sup> spectra of  $[M + H - NH_3]^+$  and  $[M + H - H_2O]^+$ , that is, the sequence  $m/z$  325  $\rightarrow$  308 (Figure 6c) and  $m/z$  325  $\rightarrow$  307 (Figure 6d), respectively. Since both MS<sup>3</sup> spectra revealed the presence of  $m/z$  290, this ion corresponded to  $[M + H - H_2O - NH_3]^+$ . The composition of the ion  $m/z$  280 in the first-generation spectrum of the protonated M324 (Figure 6a) could also be confidently assigned with the aid of the product ion profile of  $[M + H - NH_3]^+$  (Figure 6c). The (+)-ESI-MS<sup>3</sup> spectrum likewise showed the fragment ion  $m/z$  280; thus, it corresponded to the ion  $[M + H - NH_3 - CO]^+$ .

The scheme presented in Figure 7 compiles all the details from the above interpreted fragmentation pathways along with the structures of the major identified fragment ions of the protonated M324 (in dotted-lined box). In addition to the mass spectral elucidation already provided, the following analysis provided further support for the metabolite identity. Of the high-molecular-weight fragment ions ( $\geq m/z$  280), all but  $m/z$  290 produced the ion  $m/z$  181 (see Figure 6a–e), originating from the breakage of the C5–C7 bond (Figure 7). As an explanation, it was put forward that the ion  $m/z$  290 possessed a highly conjugated (aromatic) structure similar to the one of  $m/z$  289, which was formed by

dehydration of the protonated M306 (see Figure 5). The mass spectrum of  $m/z$  290, that is, MS<sup>3</sup> on  $m/z$  325  $\rightarrow$  290 (Figure 6e), exhibited one ion at  $m/z$  262 corresponding to the expulsion of CO under ring contraction, whereas the ions detected at  $m/z$  275 and 259 were believed to involve losses of radicals out of the trimethoxybenzene moiety. Here, the formation of  $m/z$  275 could occur in analogy to the production of  $m/z$  274 by  $m/z$  289 (see Figure 4b and Figure 5). With regard to the fragment  $m/z$  143 observed in the product ion spectrum of the protonated M324 (Figure 6a), cleavage of the bond C5–C7 led to the formation of a cyclohexenedione, for which a large number of tautomeric structures (enol/keto as well as imine/enamine) could be described, thus allowing efficient stabilization of the positive charge. The formation of the minor ion  $m/z$  221 (Figure 6a), in turn, was favored by the aromaticity of the benzopyrrium core (Figure 7).

To provide ultimate evidence for the identity of M306 and M324, accurate mass measurements were performed using QqTOF-MS, selecting the protonated molecules as precursor ions for (+)-ESI-MS<sup>2</sup> experiments. The results of these analyses are listed in Table 1, along with the calculated values of the postulated ion masses of the metabolites and their fragment ions, as well as the absolute mass measurement errors for each species detected. Due to fundamental differences between collision-induced dissociation, employed in the QqTOF-MS, and resonance excitation, used in the IT-MS, the MS/MS spectra obtained for the trimethoprim metabolites using these two instruments were not identical. However, most major fragment ions were observed in both spectra, and the fragment ion masses determined using the



**Table 1. Accurate Mass Measurements of Trimethoprim and Its Two Metabolites, M306 and M324, As Determined by LC/ESI-QqTOF-MS in MS/MS Mode<sup>a</sup>**

molecular ion/fragment ion	elemental composition	calcd mass ( <i>m/z</i> )	meas mass ( <i>m/z</i> )	abs. error (mDa)	DBE
Trimethoprim					
[M + H] <sup>+</sup>	C <sub>14</sub> H <sub>19</sub> N <sub>4</sub> O <sub>3</sub>	291.1457	291.1446	−1.1	7.5
Metabolite M306					
[M + H] <sup>+</sup>	C <sub>14</sub> H <sub>19</sub> N <sub>4</sub> O <sub>4</sub>	307.1406	307.1404	−0.2	7.5
[M + H − H <sub>2</sub> O] <sup>+</sup>	C <sub>14</sub> H <sub>17</sub> N <sub>4</sub> O <sub>3</sub>	289.1301	289.1313	+1.2	8.5
[M + H − H <sub>2</sub> O − •CH <sub>3</sub> ] <sup>+</sup>	C <sub>13</sub> H <sub>14</sub> N <sub>4</sub> O <sub>3</sub>	274.1066	274.1057	−0.9	9.0
[M + H − H <sub>2</sub> O − (CH <sub>3</sub> ) <sub>2</sub> ] <sup>+</sup>	C <sub>12</sub> H <sub>11</sub> N <sub>4</sub> O <sub>3</sub>	259.0831	259.0824	−0.7	9.5
[M + H − H <sub>2</sub> O − CH <sub>3</sub> − OCH <sub>3</sub> ] <sup>+</sup>	C <sub>12</sub> H <sub>11</sub> N <sub>4</sub> O <sub>2</sub>	243.0882	243.0872	−1.0	9.5
Metabolite M324					
[M + H] <sup>+</sup>	C <sub>14</sub> H <sub>21</sub> N <sub>4</sub> O <sub>5</sub>	325.1512	325.1522	+1.0	6.5
[M + H − H <sub>2</sub> O] <sup>+</sup>	C <sub>14</sub> H <sub>19</sub> N <sub>4</sub> O <sub>4</sub>	307.1406	307.1364	−4.2	7.5
[M + H − CO] <sup>+</sup>	C <sub>13</sub> H <sub>21</sub> N <sub>4</sub> O <sub>4</sub>	297.1563	297.1578	+1.5	5.5
[M + H − NH <sub>3</sub> − H <sub>2</sub> O] <sup>+</sup>	C <sub>14</sub> H <sub>16</sub> N <sub>3</sub> O <sub>4</sub>	290.1141	290.1118	−2.3	8.5
[M + H − NH <sub>3</sub> − CO] <sup>+</sup>	C <sub>13</sub> H <sub>18</sub> N <sub>3</sub> O <sub>4</sub>	280.1297	280.1344	+4.7	6.5
<i>m/z</i> 221	C <sub>12</sub> H <sub>13</sub> O <sub>4</sub>	221.0814	221.0795	−1.9	6.5
<i>m/z</i> 181	C <sub>10</sub> H <sub>13</sub> O <sub>3</sub>	181.0865	181.0855	−1.0	4.5
<i>m/z</i> 143	C <sub>4</sub> H <sub>7</sub> N <sub>4</sub> O <sub>2</sub>	143.0569	143.0596	2.7	3.5

<sup>a</sup> DBE: double bond equivalents

QqTOF-MS were determined to be within ≤5 mDa of the theoretical values (within instrument specifications for the mass range of the fragment ions), and mass accuracies of ≤5 ppm were achieved for the protonated pseudomolecular ions of trimethoprim, M306 and M324.

In conclusion, the microbial degradate M306 was unequivocally identified as α-hydroxytrimethoprim. This compound, along with metabolites originating from O-demethylation and ring N-oxidation, had been described as one of the major trimethoprim metabolites formed after administration to mammals, including dogs, rats, and humans.<sup>15,16</sup> It was also determined in *in vitro* studies as an oxidative metabolite of trimethoprim using cell culture media and microsome incubation mixtures.<sup>17</sup> The second metabolite identified in this work, M324, had not been reported in higher organisms, and thus, its formation is hypothesized to be strictly confined to the microbial community in nitrifying activated sludge.

**Environmental Relevance.** The degradation studies revealed that nitrifying sludge bacteria were capable of facilitating an oxidation of trimethoprim, a pharmaceutical which is not amenable

to biological degradation in a conventional activated sludge process. This represents an important outcome in view of the great potential of removing other polar persistent drugs from sewage and ultimately of minimizing the contamination of natural water systems. Instead of applying cost-intensive tertiary treatment technologies, such as advanced oxidation processes, the integration of biological treatments making use of nitrifying bacteria, which flourish in low organic carbon, ammonium-enriched environments, is worth consideration as an alternative strategy. Further research in this direction is needed.

#### ACKNOWLEDGMENT

This material is based upon work supported by the National Science Foundation under Grant No. 0233700. Any opinions, findings, and conclusions or recommendations expressed in this material are those of the authors and do not necessarily reflect the views of the National Science Foundation. This study was also supported by a grant from the Interdisciplinary Research and Creative Activities Fund of the University at Buffalo. S. Pérez acknowledges a postdoctoral fellowship from the Spanish Ministry of Education, Culture and Science (EX2003-0687).

Received for review January 24, 2005. Accepted April 7, 2005.

AC050141P

(15) Schwartz, D. E.; Vetter, W.; Englert, G. *Arzneim.-Forsch.* **1970**, *20*, 1867–1871.

(16) Meshi, T.; Sato, Y. *Chem. Pharm. Bull.* **1972**, *20*, 2079–2090.

(17) van't Klooster, G. A.; Kolker, H. J.; Woutersen-van Nijnanten, F. M.; Noordhoek, J.; van Miert, A. S. *J. Chromatogr.* **1992**, *579*, 354–360.